1-1-2013

An Effective Field Theory Calculation of n(p, d)γ Cross-section for Big Bang Nucleo-synthesis

Rasha Adnan Kamand
University of South Carolina

An Effective Field Theory Calculation of $n(p,d)\gamma$ Cross-section for Big Bang Nucleo-synthesis

by

Rasha Adnan Kamand

Bachelor of Science - Physics
American University of Beirut, Lebanon 2008

Submitted in Partial Fulfillment of the Requirements

for the Degree of Master of Science in

Physics

College of Arts and Sciences

University of South Carolina

2013

Accepted by:

Matthias R. Schindler, Director of Thesis

Kuniharu Kubodera, Reader

Lacy Ford, Vice Provost and Dean of Graduate Studies

Abstract

Studying the nuclear reaction $n(p,d)\gamma$ and calculating its cross-section is not only a matter of interest from theoretical particle physics point of view but also from the viewpoint of cosmology. We now know that the universe is made up of only ≈ 5 % baryonic matter. So, computing the density of baryons is of particular importance to physicists in general and cosmologists in particular. Deuterium production during Big Bang Nucleo-synthesis (BBN) is very sensitive to the density of baryons, thus baryon density can be inferred from the abundance of deuterium. In order to calculate deuterium abundance one needs to use the cross-section of $np \to d\gamma$ reaction as one of the inputs. Hence, the importance of this cross-section calculation.

In this document, a leading-order (LO) calculation of $n(p,d)\gamma$ cross-section is presented using the framework of pion-less effective field theory with dibaryon fields. The computation yielded a numerical value of $\sigma_{LO} = 494$ mb which is then compared to the experimental value.

Table of Contents

List of Figures

Chapter 1

Introduction/Motivation

The early universe was a nuclear reactor. A few minutes after the Big Bang, a series of reactions took place whereby the first light nuclei were formed. These are Deuterium (D), Tritium (^3H), Helium 3 (^3He), Helium 4 (^4He) and Lithium 7 (^7Li). The process of formation of the above nuclei is known as the Big Bang Nucleo-synthesis (BBN) which started when the universe was approximately 3 minutes old and lasted for about half an hour after the Big Bang. The first step in nucleo-synthesis is the binding of a proton p and a neutron n to build a deuteron d(the nucleus of a Deuterium atom) through the following reaction $n + p \rightarrow d + \gamma$, where γ denotes a photon.

In the following thesis, the cross-section for $np \rightarrow d\gamma$ will be calculated up to leading-order using pion-less effective field theory (EFT) with dibaryon fields. It is therefore necessary and useful to give a general overview of EFTs paying particular attention to pion-less EFT (EFT($\not\pi$)). This will be done in Chapter 3. The cross-section calculation which will be presented in details in Chapter 4 is one application of pion-less EFT. As mentioned above, in the context of BBN, deuteron formation is the first link in the chain of reactions that produce the other light elements. Furthermore, deuteron production is very sensitive to the density of baryons, so deuterium abundance gives the most accurate value for the baryon density. Calculating deuterium abundance uses the cross-section of the reaction $np \rightarrow d\gamma$. The $n(p, d)\gamma$ cross-section calculation is also a matter of interest in the field of theoretical nuclear and particle physics research. It is noteworthy to mention that further calculations have been

done where the cross-section was evaluated to higher orders using again pion-less EFT [1, 2, 3]. Moreover, the polarized np reaction $\vec{n} + \vec{p} \to d + \gamma$ has been studied within the framework of EFT to calculate some spin-dependent observables [4]. We will talk about this in a little bit more detail in the last chapter.

Now, let us begin with a discussion about BBN. But before we do that, it will be a good idea to start with a brief synopsis of the history of the universe according to the theory of the Big Bang.

Chapter 2

Nucleo-synthesis in the Early Universe

The first few elements in the periodic table were synthesized approximately three minutes after the birth of the universe at the time when the temperature was low enough to allow the formation of light nuclei through the process of nucleo-synthesis. In the course of this chapter, we will review in section one the history and stages of the universe after the "big bang" took place up until the stage of BBN, which will be discussed in the second section.

2.1 The Early Universe

How did the universe come into existence? Well, there is no one final and conclusive answer that explains the birth of our universe. A few theories have been proposed to unravel the mystery of the origin of the cosmos. The Big Bang model is the most widely accepted cosmological theory of the early universe and its development after the moment of the "big bang". It was put in proposition as the "hypothesis of the primeval atom" in 1931 by Georges Lemaitre [5], a Belgian priest and physicist, and later supported and developed by Gamow [6].

According to the Big Bang theory, the universe emerged from a "singularity", infinitely hot and dense. Why and how that happened are still unknown. The evolution of the "baby" universe directly after the instant of the "big bang" is still speculative. The reason is that we currently don't have any theory that can account for the physics

at the Planck scale which is around 1.22×10^{19} GeV. So we will not discuss what happened during the Planck era and shortly after that, but our discussion of the history of the universe will start after the so called "inflationary epoch" when the early universe is permeated with a plasma of elementary particles, namely quarks, leptons and their anti-particles and of course photons.

2.1.1 Evolution of the early universe after the quark epoch

About 10^{-6}s after the "big bang", the temperature dropped down to the point where the average interaction energy between quarks fell below the binding energy of hadrons inside which the quarks got confined. Before the formation of hadrons, it is theorized that the universe was filled with quark-gluon plasma as the temperature was too high for stable hadrons to form. The conditions that give rise to a quark-gluon plasma are still unknown; however, the strong force that binds quarks into hadrons is known to become weaker at very high temperatures, a property called "asymptotic freedom".

In what follows, I will base my description of the stages of cosmic evolution mostly on Steven Weinberg's *The First Three Minutes* [7].

At t≈0.01s after the "big bang": The temperature is around 10^{11} K, and the universe is in a state of thermodynamic equilibrium which means that there is no net flow of matter or energy. A system in thermodynamic equilibrium is characterized by a uniform temperature. The universe is dominated by a soup of matter that includes electrons (e^-), positrons (e^+), neutrinos (ν), anti-neutrinos ($\bar{\nu}$) and radiation (photons). The percentage of nucleons is small at this time, in the ratio of one nucleon for each 10^9 photons [7]. Due to the high temperature, the rate of collisions between particles is high. The neutron to proton (n/p) ratio is kept in thermal equilibrium

$(n/p \approx 1)$ due to the following two reactions

$$p + e^- \longleftrightarrow n + \nu$$

and

$$n + e^+ \longleftrightarrow p + \bar{\nu}$$

The universe continues to cool and expand.

At t≈0.12s after the "big bang": T≈ 3×10^{10} K and the state of the universe is still pretty much the same. Expansion continues and as the temperature drops further, the reaction in which neutrons turn into protons is favored because neutrons are heavier and thus easier to form lighter protons. So the (n/p) ratio is no longer equal to unity. The number of nucleons is now 38% neutrons and 62% protons.

At t≈1.10s after the "big bang": The temperature cools down to about 10^{10} K. The density is decreasing as the universe is still expanding. This falling off in the energy and density increases the mean free path of neutrinos and their anti-particles, so they are almost free particles now. The neutrinos then decouple and cease to be in thermal equilibrium with the rest of the other particles. Protons and neutrons at this stage cannot combine to form the light nuclei because the temperature is still relatively high for the nucleons to be bound.

At t≈13.83s after the "big bang": We have now reached a temperature of 3×10^9 K which is less than the threshold energy to produce electron-positron pairs. So these

particles are annihilated fast. Stable nuclei like ^4He can now be formed; however, this is not achieved during this phase. The reason behind that is the following: the production of ^4He happens gradually in a series of two-particle reactions starting with deuteron production $n + p \rightarrow d + \gamma$, but the deuteron nucleus is loosely bound. So at the current temperature, as soon as deuteron nuclei are formed, they are quickly dissociated by the inverse reaction $d + \gamma \longrightarrow n + p$. Thus, heavier nuclei are not created.

At t≈ 3 minutes after the "big bang": It is approximately 10^9 K at this period, and our universe is mainly filled with neutrinos, their anti-particles and photons. A reaction which further decreases the number of neutrons has started to take place: the decay of free neutrons ($n \longrightarrow p + e^- + \bar{\nu}$). The (n/p) ratio is now around 1:7. The universe is still hot for the "deuteron bottleneck" to be overcome, in other words, deuteron nuclei continue to be broken up once they are created.

A little later than three minutes, the temperature becomes low enough for deuteron nuclei to form and not be destroyed, so then the phase of nucleo-synthesis "officially" commences! But as I promised earlier in the "Motivation", Big Bang Nucleo-synthesis will be discussed in a somewhat thorough manner, and the upcoming section will be devoted to that purpose.

2.1.2 Observational evidence of the Big Bang

The Big Bang model for the evolution of the early universe is supported by what is known as the *four pillars*. The first is the **expansion of the universe**; in 1929, Edwin Hubble was the first to observe that galaxies are receding away from us and from one another. The **cosmic microwave background** (**CMB**) which was discovered by

Penzias and Wilson is a relic of the big bang. The CMB is a "leftover" radiation from the early stages of the development of the universe. The third supporting evidence is the **abundance of the first light elements** as predicted by BBN. The calculated abundances of the primordial elements are in close agreement with their measured values. **Galactic evolution** as predicted and explained by the Big Bang theory agrees with the observations of the formation and distribution of galaxies. This constitutes the fourth pillar of the Big Bang model.

2.2 Big Bang Nucleo-synthesis

Before we talk about the physics of primordial nucleo-synthesis, it would be informative to mention very briefly the history of the theory of BBN.
In 1942, G. Gamow proposed that the elements that we know today had their origins during the evolution of the universe after the "big bang". In their seminal 1948 paper entitled "The Origin of Chemical Elements", Alpher, Bethe and Gamow suggested that elements of the periodic table were formed in a series of neutron capture reactions a few minutes after the birth of our universe [6]. However, further research showed that the big bang was responsible for the production of the first few elements only, mainly ^4He [8], the reason being that nuclei with mass numbers 5 and 8 are unstable and the Coulomb repulsion dominates as the temperature drops. A few years later, two independent research papers were published explaining that the remaining elements of the periodic table (with high mass and atomic numbers) were created in stellar reactions [9, 10].

The framework of BBN was used to calculate and predict the primeval abundances of the light elements ^2H, ^3He, ^4He and ^7Li which turned out to be in agreement with the observed values [11, 12, 13, 14]. More importantly, calculations done using deuterium abundance succeeded in finding an upper limit to the baryon density in

the universe [15]. BBN has been one of the pillars of the Big Bang model and a probe of not only fundamental but also new physics [16].

2.2.1 The physics processes of BBN

At T $\gg$ 1 MeV, thermodynamic equilibrium dominated the universe. Among other factors, the nuclear reactions which maintained thermodynamic equilibrium are

$$n + \nu_e \leftrightarrow p + e^-,$$

$$n + e^+ \leftrightarrow p + \bar{\nu_e},$$

$$n \leftrightarrow p + e^- + \bar{\nu_e},$$

The neutron-to-proton ratio was fixed at $(n/p) \simeq e^{-\triangle m/T} \approx 1$ where $\triangle m = 1.293$ MeV is the neutron-proton mass difference.

As the universe expanded and cooled down to around 1 MeV, the neutrinos and their anti-particles, which were kept in thermal equilibrium also via weak interaction, stopped interacting with the other particles (mainly e^+ and e^-). So the weak interactions are said to"freeze-out", and the (n/p) ratio also froze at about (1/6). At T$\approx$1 MeV, nucleo-synthesis kind of began with the reaction

$$n + p \leftrightarrow d + \gamma.$$

Deuteron started to form, but due to the high number density of photons (n_γ) relative to that of nucleons (n_B), $[\eta^{-1} = (n_\gamma/n_B) \approx 10^{10}]$, the deuteron nuclei were rapidly photo-dissociated. Deuteron production was delayed and BBN did not kickoff until the temperature fell below the deuteron binding energy of 2.2 MeV.

The dominant reaction at about 0.5 MeV was the free neutron decay which has a

half-life of $t_{1/2} \approx 882s$. This further dropped the (n/p) fraction to approximately $(1/7)$ by the time of nucleo-synthesis. It is important to know that the presence of free neutrons was one of the necessary conditions for synthesizing the first few light nuclei.

When the temperature reached ≈ 0.1 MeV, the universe was a few minutes old, a little more than 3 minutes. At last, deuteron nuclei began to form via neutron capture:

$$n + p \rightarrow d + \gamma,$$

without being dissociated, the reason being that the number of photons per baryon with energies above the deuteron binding energy was well below unity. And so the nucleo-synthesis chain started with the above reaction (deuteron production reaction), and the other light nuclei were formed by a series of two-body, neutron-capture reactions. Once deuteron formation took place, other nuclear reactions proceeded to produce other light nuclei mainly ^4He that has a higher binding energy ($E_B \cong 28$ MeV) than deuteron ($E_d \cong 2.2$ MeV). Here are two possible sets of reactions (photo-reactions) that ultimately produce Helium 4:

$$d + n \rightarrow {}^3H + \gamma,$$

$$^3H + p \rightarrow {}^4He + \gamma,$$

$$d + p \rightarrow {}^3He + \gamma,$$

$$^3He + n \rightarrow {}^4He + \gamma.$$

Due to the instability of nuclei with mass number 5, there was another bottleneck at ^4He. Among the few light nuclides produced by BBN, ^4He is the most tightly bound which resulted in almost all neutrons bound in ^4He nuclei. Despite the bottleneck

at mass number 5, a few reactions where the Coulomb interaction got suppressed managed to overcome the gap and form ^7Li and ^7Be. As the temperature fell below $\approx$ 30 keV, and approximately 20 minutes passed since the"big bang", Coulomb repulsion and the near absence of free neutrons prevented any further reactions. Consequently another gap appeared at mass number 8 (mass 8 nuclei are also unstable), and no heavier nuclides were created until the first stars were born. This marked the end of the primordial nuclear reactor and thus of the BBN phase.

Chapter 3

Effective Field Theory (EFT)

The main part of my thesis is the calculation of the $n(p,d)\gamma$ cross-section which is presented in Chapter 4. The cross-section is calculated up to leading order (LO) applying the framework of pion-less EFT with dibaryon fields. Before going into the details of my calculation, I devote this chapter to introduce the general audience to EFTs. I should note that my discussion on EFTs is by no means a thorough treatment of this topic. I will just touch the surface trying to summarize the general idea behind EFT and explain the main points. And so the interested general reader can get more detailed and rigorous explanation/analysis in the following references [21, 22, 23, 24, 25, 26] and many others.

Let's start our discussion by first asking the question: In Physics, what is an **effective theory**? Well, I think that almost all physicists would agree that the theories in Physics which we know of so far are actually *effective theories* except a THEORY OF EVERYTHING which has not been found yet! Nature and consequently the world that we live in can be divided into different energy or length scales ranging from the Planck scale ($\approx 1.6 \times 10^{-35}$ m) to the length scales of galaxies. In each length/energy range, physicists find a suitable or useful description of the important or relevant physics processes (dynamics) taking place. The reason behind that lies in the basic principle which states that the dynamics at long distances (low energies) do not depend on the details of what is happening at short distances (high energies). And so, this suitable description of the relevant physics at a particular energy scale is called *"an effective*

theory". The key idea behind an effective theory is to set the parameters that are very small (negligible), in comparison to our physical quantities of interest, to zero and set those which are very large to infinity; the effects of these parameters can then be treated as small perturbations. In other words, an effective theory is valid below a certain energy scale Λ and thus in a limited energy range. It is a systematic approximation to a more "fundamental" theory which is valid at all energies including arbitrarily high energies.

It is certainly not essential or mandatory to use an effective theory in cases where the more fundamental theory is known and established, but it is actually more convenient and simpler to do so most of the times. One example is Newtonian Classical Mechanics. We are taught classical mechanics as developed by Newton in high school and later in college we learn about special relativity. In fact, Newtonian mechanics is an effective theory valid in the range of small velocities compared to the speed of light c. However, physicists encounter situations where they don't know what the fundamental theory is or whether it exists. It could also be the case that the more basic theory is known to exist but is very difficult to solve. Therefore, in these cases, it is necessary to formulate an effective theory and employ it in order to find a useful and simple picture of the important physics. For instance, theoretical particle physicists, till the present moment, have not been able to solve Quantum Chromo-dynamics (QCD), the theory of the strong interaction, at low energies. So a theoretical framework known as Chiral Perturbation Theory (ChPT) was developed to analyze QCD at low energies. ChPT is the QCD low-energy effective theory.

3.1 Effective Field Theory Techniques

ChPT, mentioned above, is one example of an *effective field theory* employed in theoretical nuclear/particle physics. An EFT is a field theory framework appropriate for the description of low-energy physical phenomena. When one says low-energy, it is meant low with respect to some energy scale or energy cutoff Λ. In an EFT, only the pertinent degrees of freedom (d.o.f) are taken into account, those with mass $m \ll \Lambda$. The heavier fields whose mass $M \gg \Lambda$ are eliminated out of the action. In constructing an EFT, theoretical physicists usually use one of the two general approaches, the bottom-up or the top-down. The top-down approach starts with the action of the high-energy theory, and the effective action is obtained by systematically integrating out the high-energy degrees of freedom. The other approach (bottom-up) constructs the effective theory action without relying on a "more fundamental" action because it is unknown. So, the effective action in the latter approach is built from scratch. In both procedures, the effective Lagrangian which describes the EFT is an expansion in terms of a sum of local operators (the sum is infinite)

$$\mathcal{L}_{eff} \;=\; \sum_i c_i \, O_i \; .$$

These operators O_i that are included in the effective Lagrangian must be consistent with the symmetries of the high-energy theory and, as mentioned above, are constructed from the light fields. The coefficients c_i are the couplings. They carry information on the high-energy d.o.f which have been integrated out.

As mentioned in the above paragraph, the most general effective Lagrangian that is consistent with the symmetries of the underlying theory consists of an infinite number of terms. Of course, it wouldn't be any easier to use an EFT if we had to compute an infinite number of terms. This isn't an achievable task. The reason why the EFT approach is useful lies in the fact that when calculating a physical observ-

able, we only require a certain **finite** accuracy of our results. This leads us to the concept of power counting. EFT corresponds to an expansion in $\frac{q}{\Lambda}$ where q stands for energy, mass or momentum such that $q \ll \Lambda$. Power counting basically helps us determine the order up to which we need to expand so as to achieve a specific accuracy (see e.g. Ref.[34]).

In field theories, while calculating observables in physical processes, one may encounter divergent integrals. Measurable physical quantities cannot be infinite. These divergences appear as intermediate stages in field theory calculations, and they eventually get cancelled out yielding finite values for physical quantities. So, certain techniques were developed in order to deal with these infinities. Treating the divergences is a two-step process starting with "regularization" and then "re-normalization". In the first step, we "regulate" the divergent integrals, i.e. we make the apparent divergences look finite by introducing what is called a "regulator". In doing so, we can then manipulate these integrals. In quantum field theory, there are a few regularization methods such as cut-off regularization, Pauli-Villars, dimensional regularization (DimReg), etc. More detailed discussion and examples can be found in [27, 28]. Later in this chapter, I will present a calculation using dimensional regularization.

After regularization, the divergent integral denoted by $\mathbf{I}$ is parametrized in terms of the regulator, which will be denoted by β. So $\mathbf{I} \equiv \mathbf{I}(\beta)$, and the divergent behavior is now embedded in the regulator β. The next step would be to actually get rid of the infinities via what is known as "re-normalization". Theoretical physicists employ different re-normalization schemes, minimal subtraction (MS), modified minimal subtraction ($\overline{MS}$), power divergence subtraction (PDS), etc. I will not be discussing these different re-normalization schemes here. Re-normalization theory is a field of study on its own. The main idea behind re-normalization in quantum field theories is

the following: the divergences coming from the integrals (loop diagrams in field theories) can be removed by an appropriate redefinition of the parameters (bare couplings c_{i_0}) in the Lagrangian density.

$$c_{i_0} \longrightarrow c_{i_R} = c_{i_0} + \delta c_i(\beta). \tag{3.1}$$

The infinities from the integrals are absorbed by $\delta c_i(\beta)$. So, the parameters c_{i_0} get "re-normalized" to c_{i_R} which are finite. c_{i_R} are the observed values that get measured in experiments.

3.2 Pion-less EFT with Dibaryon Fields

As an example of EFT, I will discuss EFT($\not\pi$) with the use of dibrayon fields. Before I go into the details of the theory, I should note that this will be a useful example in which I calculate the dressed dibaryon propagator employing dimensional regularization [38] and the PDS scheme [33]. The dressed dibaryon propagator will then be used in the calculations of the upcoming chapter.

Pions play an important role in mediating the nucleon-nucleon (NN) interaction; however, at low enough energies (momenta $p \ll m_\pi$), the pions are integrated out of the effective Lagrangian as heavy fields. So, in EFT($\not\pi$), the only relevant degrees of freedom are the nucleons. In other words, EFT($\not\pi$) is a low-energy theory suitable to describe and study reactions (at momenta $p \ll \frac{1}{R}$) between particles with a short-range (R) interaction that exhibits a large scattering length. The framework of EFT($\not\pi$) has been employed to study many physical phenomena such as radiative neutron capture ($np \to d\gamma$) in the context of BBN [2, 29], electromagnetic form factors of the deuteron [1, 30], and other processes that involve electro-weak gauge fields. For a more detailed discussion of EFT($\not\pi$), please see [26].

When dealing with the deuteron, it was shown (see references [31, 32]) that it's more convenient to introduce an auxiliary field called dibaryon (that can be thought of as a bound state of two nucleons), denoted by t, which simplifies computations. In Chapter 4, I will calculate the cross-section of $np \to d\gamma$ up to LO using EFT($\not\pi$) with the dibaryon field. The calculation involves two LO Feynman diagrams which are schematic drawings showing interaction vertices and propagators. So, to carry out the calculation, we first need to find the nucleon and dibaryon propagators and also compute the Feynman rules for the vertices. The reason why I present the dressed dibaryon propagator calculation now is that it involves a loop integral that needs to be regularized and then re-normalized, so it is a good example relevant to this chapter.

3.2.1 Dressed Dibaryon Propagator

The dibaryon propagator that enters in the cross-section calculation of the reaction $n(p,d)\gamma$ is the "dressed" (full) propagator. The bare dibaryon propagator gets dressed by nucleon bubbles (loops) to all orders (see Figure 3.1). Let me denote the bare propagator by S_d and the dressed propagator by D. S_d can be derived from the kinetic term for the dibaryon field in the Lagrangian. The Lagrangian density describing the dynamics in both the ${}^3S_1$ and ${}^1S_0$ channels is [32]

$$\begin{aligned}\mathcal{L}^d_{PC} = {} & N^\dagger(i\partial_0 + \frac{\vec{\partial}^2}{2M})N - t_i^\dagger(i\partial_0 + \frac{\vec{\partial}^2}{4M} - \triangle^{({}^3S_1)})t_i \\ & - g^{({}^3S_1)}[t_i^\dagger N^T P_i^{({}^3S_1)} N + h.c.] - s_a^\dagger(i\partial_0 + \frac{\vec{\partial}^2}{4M} - \triangle^{({}^1S_0)})s_a \\ & - g^{({}^1S_0)}[s_a^\dagger N^T P_a^{({}^1S_0)} N + h.c.] + \frac{e}{2M} N^\dagger \left(\kappa_0 + \tau_3\kappa_1\right)\vec{\sigma}\cdot\vec{B}N\end{aligned} \tag{3.2}$$

Here, N and $N^\dagger$ are the nucleon fields, M is the nucleon mass, κ_0 and κ_1 are the

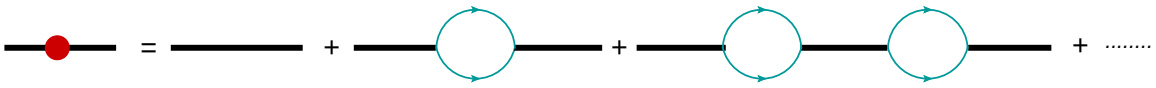

Figure 3.1 Dressed Dibaryon Propagator

isoscalar and isovector nucleon magnetic moments, $g^2 = \frac{8\pi}{M^2 r}$ and $\triangle = \frac{2}{Mr}(\frac{1}{a} - \mu)$ are the couplings with r and a denoting the effective range and scattering length, respectively, while μ is a re-normalization scale that appears later in re-normalizing the loop integral.

The dibaryon fields in the ${}^3S_1$ and ${}^1S_0$ channels are represented by t_i and s_a, respectively.

$$P_a^{({}^1S_0)} = \frac{1}{\sqrt{8}}\tau_2\tau_a\sigma_2, \tag{3.3}$$

$$P_i^{({}^3S_1)} = \frac{1}{\sqrt{8}}\tau_2\sigma_2\sigma_i \tag{3.4}$$

are the normalized projection operators where τ_a and σ_i, $a, i = 1, 2, 3$, are the Pauli isospin and spin matrices, respectively.

As mentioned above, the bare dibaryon propagator can be derived from the dibaryon kinetic term,

$$\langle t_i^\dagger | (-t_a^\dagger)(i\partial_0 + \frac{\vec{\partial}^2}{4M} - \triangle) t_b \delta_{ab} | t_j \rangle \ . \tag{3.5}$$

So this gives

$$S_d(p_0, \vec{p}_{total}) = \frac{\delta_{ij}}{-p_0 + \frac{\vec{p}_{total}^2}{4M} + \triangle + i\varepsilon} \ , \tag{3.6}$$

(note that the convention I am using is that in a Feynman diagram, a line stands for $i\times$propagator).

As shown in Figure 3.1, the dressed dibaryon propagator is obtained by summing an infinite number of nucleon loops at all orders. The reason we do this infinite

re-summation is explained by power counting [32]. The bare dibaryon propagator $S_d \sim Q^{-2}$ where Q is a small momentum expansion parameter. Each vertex is $\sim Q^{1/2}$, and each loop contributes a factor of Q. So, by applying the latter power counting scheme, every diagram in figure 3.1 counts as Q^{-2}. Therefore, the nucleon bubbles must be summed to all orders.

The calculation involves computing the nucleon loop integral which will be denoted by I_{loop}. This integral will be regularized by DimReg then re-normalized by PDS. Although we are summing an infinite number of terms, we notice that this sum is a geometric series which has a closed form

$$iD = iS_d\left(\frac{1}{1 - i\ I_{loop}\ S_d}\right) . \tag{3.7}$$

Loop integral I_{loop} calculation

We first need to take a look at the loop diagram below. Let me note that we are

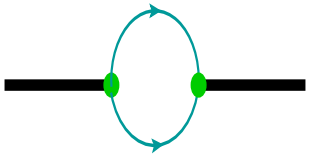

Figure 3.2 Nucleon bubble

working in the center of mass frame, and the incoming dibaryon has total energy E and zero momentum $(E, \vec{0})$. This energy gets distributed between the two nucleons where one has $(\frac{E}{2} + p_0, \vec{p})$, and the other has $(\frac{E}{2} - p_0, -\vec{p})$, where p_0 and $\vec{p}$ are loop/integration momenta. As seen in figure 3.2, there are two interaction vertices which we need to compute. The "Feynman rules" give the following vertices:

a) Incoming dibaryon to two outgoing nucleons:

$$-iy\langle N_A^\dagger N_B^\dagger \mid N_R^\dagger P_{RS}^{j\dagger} N_S^\dagger t_j \mid t_i\rangle = -iy P_{AB}^{i\dagger}, \tag{3.8}$$

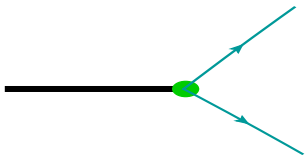

Figure 3.3 Dibaryon to two nucleons vertex

b) Two incoming nucleons to outgoing dibaryon:

$$-iy\langle t_i^\dagger \mid t_j^\dagger N_R P_{RS}^j N_S \mid N_A N_B\rangle = -iy P_{AB}^i, \tag{3.9}$$

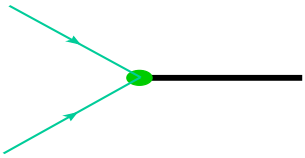

Figure 3.4 Two nucleons to dibaryon vertex

Let me note that the A, B, R, and S are spin and isospin indices carried by the nucleon fields, that is A=(a,α), B=(b,β), etc. where a,b and α,β, etc. are the isospin and spin indices, respectively. To avoid confusion, let me point out that the 'y' appearing in equations (3.8) and (3.9) is a general coupling that gets replaced later by the appropriate coupling constant in the different $^3S_1$ and $^1S_0$ channels.
Also needed is the nucleon propagator which can be derived from the nucleon kinetic term in the Lagrangian which gives

$$S_N(k_0, \vec{k}) = \frac{1}{k_0 - \frac{\vec{k}^2}{2M} + i\epsilon} \ . \tag{3.10}$$

We are now in good shape to calculate the loop integral. So,

$$\begin{aligned} I_{loop} &= (-2iyP_{AB}^{i\dagger})\,(-iyP_{AB}^{j}) \int \frac{d^4p}{(2\pi)^4} \frac{i}{\frac{E}{2}+p_0-\frac{\vec{p}^2}{2M}+i\epsilon}\,\frac{i}{\frac{E}{2}-p_0-\frac{\vec{p}^2}{2M}+i\epsilon} \\ &= -2y^2 P_{AB}^{i\dagger}\; P_{BA}^{j} \int \frac{d^4p}{(2\pi)^4} \frac{1}{\frac{E}{2}+p_0-\frac{\vec{p}^2}{2M}+i\epsilon}\,\frac{1}{\frac{E}{2}-p_0-\frac{\vec{p}^2}{2M}+i\epsilon} \\ &= -2y^2 Tr(P^{i\dagger}P^{j}) \int \frac{d^4p}{(2\pi)^4} \frac{1}{\frac{E}{2}+p_0-\frac{\vec{p}^2}{2M}+i\epsilon}\,\frac{1}{\frac{E}{2}-p_0-\frac{\vec{p}^2}{2M}+i\epsilon} \\ &= -2y^2(\frac{1}{2}\delta^{ij}) \int \frac{d^4p}{(2\pi)^4} \frac{1}{\frac{E}{2}+p_0-\frac{\vec{p}^2}{2M}+i\epsilon}\,\frac{1}{\frac{E}{2}-p_0-\frac{\vec{p}^2}{2M}+i\epsilon} \\ &= y^2\delta^{ij} \int \frac{d^4p}{(2\pi)^4} \frac{1}{\frac{E}{2}+p_0-\frac{\vec{p}^2}{2M}+i\epsilon}\,\frac{1}{-\frac{E}{2}+p_0+\frac{\vec{p}^2}{2M}-i\epsilon}\,. \end{aligned} \tag{3.11}$$

The factor of '2' is a symmetry factor coming from the two different ways of connecting the nucleon lines to form the full loop. Note that I now used 'p' instead of 'k' for the nucleon momentum, but that doesn't really matter since the 'k' that appeared in the propagator S_N is just a dummy variable.

The above integral diverges linearly in 4 dimensions, so we use DimReg (see e.g. Ref [34]) to regulate this divergence. Going to n dimensions, we get

$$\begin{aligned} I_n &= (\frac{\mu}{2})^{4-n} \int \frac{d^np}{(2\pi)^n} \frac{1}{\frac{E}{2}+p_0-\frac{\vec{p}^2}{2M}+i\epsilon}\,\frac{1}{-\frac{E}{2}+p_0+\frac{\vec{p}^2}{2M}-i\epsilon} \\ &= (\frac{\mu}{2})^{4-n} \int \frac{dp_0d^{n-1}p}{(2\pi)^n} \frac{1}{\frac{E}{2}+p_0-\frac{\vec{p}^2}{2M}+i\epsilon}\,\frac{1}{-\frac{E}{2}+p_0+\frac{\vec{p}^2}{2M}-i\epsilon} \\ &= (\frac{\mu}{2})^{4-n} i \int \frac{d^{n-1}p}{(2\pi)^{n-1}} \frac{1}{E-\frac{\vec{p}^2}{M}+i\epsilon} \\ &= -iM(\frac{\mu}{2})^{4-n} \int \frac{d^{n-1}p}{(2\pi)^{n-1}} \frac{1}{\vec{p}^2-ME-i\epsilon}\,. \end{aligned} \tag{3.12}$$

Performing the angular integration first using $\int_0^\pi d\theta \sin^m(\theta) = \frac{\sqrt{\pi}\Gamma(\frac{m+1}{2})}{\Gamma(\frac{m+2}{2})}$, we arrive at the following expression

$$I_n = -iM(\frac{\mu}{2})^{4-n} \frac{(2\pi)\pi^{\frac{n-3}{2}}}{(2\pi)^{n-1}\Gamma(\frac{n-1}{2})} \int_0^\infty dp \frac{p^{n-2}}{\vec{p}^2+(-ME-i\epsilon)}\,. \tag{3.13}$$

We now let $t = \frac{p^2}{-ME-i\epsilon}$,

$$I_n = \frac{1}{2}(-ME-i\epsilon)^{\frac{n-3}{2}} \int dt \frac{t^{\frac{n-1}{2}}-1}{t+1}\,. \tag{3.14}$$

Using $B(x,y) = \int_0^\infty \, dt \frac{t^{x-1}}{(1+t)^{x+y}} = \frac{\Gamma(x)\Gamma(y)}{\Gamma(x+y)}$, we finally arrive at

$$I_n = -iM(\frac{\mu}{2})^{4-n}(-ME - i\epsilon)^{\frac{n-3}{2}}(4\pi)^{\frac{1-n}{2}}\Gamma(\frac{3-n}{2}) \; . \tag{3.15}$$

Notice that the above integral is divergent for n=3. In order to re-normalize the integral, we apply the Power Divergence Subtraction (PDS) scheme where the residue of the pole of the Gamma fucntion at n=3 is subtracted from the integral for n=4 [33]. So, one has to find the residue of $\Gamma(\frac{3-n}{2})$. To do this, we use $\Gamma(z+1) = z\Gamma(z)$ to rewrite

$$\Gamma(\frac{3-n}{2}) = \frac{2}{3-n}\Gamma(1 + \frac{3-n}{2}) \; . \tag{3.16}$$

Let $\varepsilon = 3 - n$, then we have $\Gamma(\frac{\varepsilon}{2}) = \frac{2}{\varepsilon}\Gamma(1 + \frac{\varepsilon}{2})$. For small ε, we expand $\Gamma(1 + \frac{\varepsilon}{2})$ in a Taylor series to get

$$\Gamma(\frac{\varepsilon}{2}) = \frac{2}{\varepsilon} + \Gamma'(1) + \frac{\varepsilon}{2}\Gamma''(1) + O(\varepsilon^2) \; . \tag{3.17}$$

We also expand $(-ME - i\epsilon)^{\frac{\varepsilon}{2}}$ by rewriting it as

$$(-ME - i\epsilon)^{\frac{\varepsilon}{2}} = \exp[\frac{\varepsilon}{2}\ln(-ME - i\epsilon)] = 1 + \frac{\varepsilon}{2}\ln(-ME - i\epsilon) + O(\varepsilon^2) \; . \tag{3.18}$$

Combining terms together we arrive at the residue of the Gamma function at n=3 which I will denote by

$$\delta I = -i\mu\frac{M}{4\pi} \; . \tag{3.19}$$

Going back to n=4,

$$I = i\frac{M}{4\pi}(-ME - i\epsilon)^{\frac{1}{2}} \; . \tag{3.20}$$

Now, in the CM frame, each nucleon has energy $\frac{\vec{p}^2}{2M}$, so the total energy is $E = \frac{\vec{p}^2}{M} \Longrightarrow$ $p = \sqrt{ME}$, then $(-ME - i\epsilon)^{\frac{1}{2}} = i\sqrt{ME + i\epsilon}$ which for $\epsilon \to 0$ gives $i\sqrt{ME} = ip$ Finally,

$$\begin{aligned} I^{PDS} &= i\frac{M}{4\pi}(ip) - (-i\mu\frac{M}{4\pi}) \\ &= i\frac{M}{4\pi}(\mu + ip) \; . \end{aligned} \tag{3.21}$$

Then the final result for I_{loop}^{PDS} is

$$\begin{aligned} I_{loop}^{PDS} &= y^2 I^{PDS} \\ &= iy^2 \frac{M}{4\pi}(\mu + ip) \ . \end{aligned} \tag{3.22}$$

Now we go back to the equation for the dressed dibaryon propagator.

$$iD = iS_d(\frac{1}{1 - i\ I_{loop}\ S_d}) \tag{3.23}$$

Having calculated I_{loop}^{PDS}, we can put the pieces together and find the expression for the full (or dressed) dibaryon propagator.

$$\begin{aligned} iD &= iS_d(\frac{1}{1 - i\ I_{loop}^{PDS}\ S_d}), \\ D &= \frac{1}{-p_0 + \frac{\vec{p}_{total}^{\,2}}{4M} + \Delta + i\epsilon} \ \frac{1}{1 + y^2 \frac{M}{4\pi}(\mu + ip) \ \frac{1}{-p_0 + \frac{\vec{p}_{total}^{\,2}}{4M} + \Delta + i\epsilon}} \\ &= \frac{1}{-p_0 + \frac{\vec{p}_{total}^{\,2}}{4M} + \Delta + i\epsilon + y^2 \frac{M}{4\pi}(\mu + ip)}. \end{aligned} \tag{3.24}$$

In CM frame, $\vec{p}_{total} = \vec{0}$, then we get

$$\begin{aligned} D(p_0) &= \frac{1}{-p_0 + \Delta + y^2 \frac{M}{4\pi}\mu + y^2 \frac{M}{4\pi} ip} \\ &= \frac{4\pi}{My^2} \frac{1}{\mu + \frac{4\pi}{My^2}\Delta - \frac{4\pi}{My^2} p_0 + ip} \ . \end{aligned} \tag{3.25}$$

Knowing that $p_0 = E$ and $p = \sqrt{ME}$, we find that

$$D(E) = \frac{4\pi}{My^2} \frac{1}{\mu + \frac{4\pi}{My^2}\Delta - \frac{4\pi}{My^2} E + i\sqrt{ME}} \ . \tag{3.26}$$

Calculating the deuteron wavefunction re-normalization

I will go one extra step and calculate the deuteron wavefunction re-normalization denoted by Z_d. The reason I do this is because we need Z_d in the next chapter to

compute the invariant amplitude for $n(p,d)\gamma$.

The dressed dibaryon propagator can be written as

$$D(E) = \frac{Z(E)}{E+B}, \tag{3.27}$$

where B is the deuteron binding energy and $Z(-B) \equiv Z_d$.

Now,

$$\left.\frac{\partial D^{-1}(E)}{\partial E}\right|_{E=-B} = \left.\Big[\frac{1}{Z(E)} + (E+B)\frac{1}{Z^2(E)}\frac{\partial Z(E)}{\partial E}\Big]\right|_{E=-B} = \frac{1}{Z_d}. \tag{3.28}$$

So we get,

$$Z_d = \left[\left.\frac{\partial D^{-1}(E)}{\partial E}\right|_{E=-B}\right]^{-1}. \tag{3.29}$$

The inverse of the dressed dibaryon propagator is

$$D^{-1}(E) = \frac{My^2}{4\pi}(\mu + \frac{4\pi}{My^2}\Delta - \frac{4\pi}{My^2})E + i\sqrt{ME}. \tag{3.30}$$

Then

$$\frac{\partial D^{-1}(E)}{\partial E} = -1 + \frac{i}{r\sqrt{ME}}, \tag{3.31}$$

where I have used $y^2 = \frac{8\pi}{M^2 r}$ [26].

So we get,

$$\left.\frac{\partial D^{-1}(E)}{\partial E}\right|_{E=-B} = \frac{1 - r\sqrt{MB}}{r\sqrt{MB}}. \tag{3.32}$$

And finally, we arrive at

$$Z_d = \frac{r\sqrt{MB}}{1 - r\sqrt{MB}}. \tag{3.33}$$

We're now ready to calculate, in the upcoming chapter, the cross-section of $n(p,d)\gamma$ up to leading order (LO) employing the framework of EFT($\not\pi$) with dibaryon fields (dEFT($\not\pi$)).

Chapter 4

LO $np \longrightarrow d\gamma$ cross-section in dEFT($\not\pi$)

As promised previously, the details of the cross-section calculation of $n(p,d)\gamma$ will be presented in this chapter. The computation is done in the framework of EFT($\not\pi$) with the use of dibaryon fields. The Lagrangian density is given in equation (3.2). The cross-section is

$$\sigma \sim \Sigma\, |\mathcal{M}|^2 \tag{4.1}$$

where the summation is over spin and isospin, and $\mathcal{M}$ is the invariant amplitude of $np \longrightarrow d\gamma$ which can be parametrized as follows [35]

$$\mathcal{M} = eXN^T\tau_2\sigma_2[(\vec{\sigma}\cdot\vec{q})(\vec{\varepsilon}^*_{(d)}\cdot\vec{\varepsilon}^*_{(\gamma)}) - (\vec{\sigma}\cdot\vec{\varepsilon}^*_{(\gamma)})(\vec{q}\cdot\vec{\varepsilon}^*_{(d)})]N + ieY\epsilon^{ijk}\varepsilon^{*i}_{(d)}q^j\varepsilon^{*k}_{(\gamma)}(N^T\tau_2\tau_3\sigma_2 N) \tag{4.2}$$

where $\vec{\varepsilon}_{(d)}$ and $\vec{\varepsilon}_{(\gamma)}$ are the polarization vectors of the deuteron and photon, respectively, $\vec{q}$ is the outgoing photon momentum, N^T and N are the nucleon fields, and $e > 0$ is the absolute value of the electron charge.

Our calculation is up to LO. The X-term appearing in Eq. (4.2) is higher order and is thus not taken into consideration.

At leading order (LO), only two diagrams (figure 4.1) contribute to the amplitude Y appearing in equation (4.2). The first is a tree-level diagram and the second involves a one-loop integral.

To start, we first need the interaction vertices, the nucleon and the dressed dibaryon propagators, S_N and D, respectively. Fortunately, we have calculated most of these in the previous chapter. The interaction vertices are given by equations (3.8)

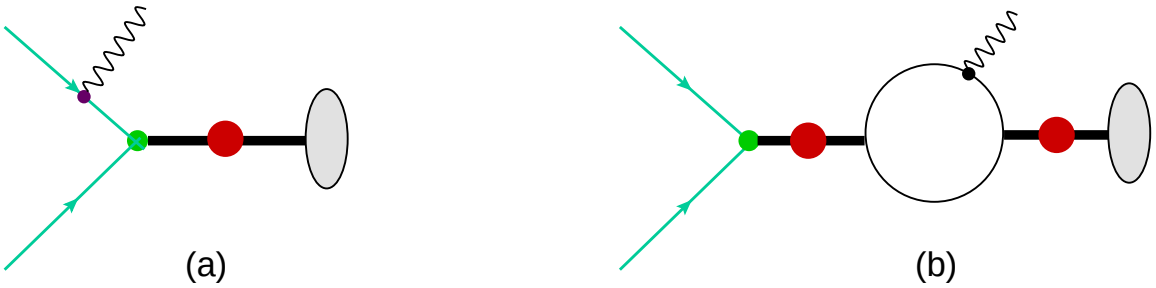

Figure 4.1 Leading-order (LO) diagrams contributing to the $np \longrightarrow d\gamma$ cross-section. Green solid lines denote nucleons, thick black lines denote dressed dibaryons, and wavy lines denote photons. The small purple circle stands for the photon coupling to the nucleon magnetic moment, and the gray oval for the deuteron interpolating field.

and (3.9). S_N and D are given by equations (3.10) and (3.26), respectively. We still need to compute one more interaction vertex (figure 4.2):

Incoming nucleon to outgoing photon and nucleon:

$$\langle\, N^\dagger A_m\,(q)\mid \frac{ie}{2M} N^\dagger\,(\kappa_0+\tau_3\kappa_1)\,\vec{\sigma}\cdot\vec{B}\;N\mid N\rangle = \frac{e}{2M} q_j\delta_{km}\,(\kappa_0+\tau_3\kappa_1)\,\sigma_i\epsilon_{ijk}, \quad (4.3)$$

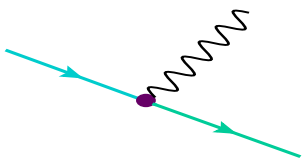

Figure 4.2 Photon vertex

where $\vec{\sigma}\cdot\vec{B} = \sigma_i\epsilon_{ijk}\partial_j A_k$, $\vec{B} = \vec{\nabla}\times\vec{A}$, A_m is the outgoing photon field and q_j is the outgoing photon momentum.

At this point, we have all the "ingredients" to start our calculation.

4.1 LO calculation of the amplitude Y

At LO, the amplitude Y appearing in equation (4.2) has a tree-level contribution and a one-loop integral contribution. We will first compute the tree-level diagram (figure 4.1 (a)) and then the one-loop integral (figure 4.1 (b)).

Tree-level contribution: diagram (a) in figure 4.1

The deuteron is in a ${}^3S_1$ state, and the photon is coupled to the nucleon through a magnetic interaction vertex. Therefore, the incoming nucleons are in a relative ${}^1S_0$ state. So we can write

$$i\mathcal{M}_{(a)} = 4\sqrt{Z_d}\,\varepsilon^{*^i}_{(d)}\,(-ig^{({}^3S_1)}\,P^i_{A'B})N^T_B\,\frac{i}{(-B)}\,\frac{e}{2M}q_j\delta_{km}\,(\kappa_0+\tau_3\kappa_1)\,\sigma_p\epsilon_{pjk}\,\varepsilon^{*^m}_{(\gamma)}\,N_A, \tag{4.4}$$

where subscripts A', A and B are spin-isospin indices, and B is the binding energy of the deuteron (also the energy of the outgoing photon). The factor of 4 is a symmetry factor.

Notice that there are two contributions, one from κ_0 and the other from κ_1. So, there will be

$$\begin{aligned}(A)\;\; P^i_{A'B}\tau_3\kappa_1\sigma_p\epsilon_{pjk} &= \frac{1}{\sqrt{8}}\sigma_2\sigma_i\tau_2\tau_3\kappa_1\sigma_p\epsilon_{pjk}\\ &= \frac{1}{\sqrt{8}}\sigma_2\tau_2\tau_3\kappa_1(\delta_{ip}+i\epsilon_{ipl}\sigma_l)\epsilon_{pjk}.\end{aligned} \tag{4.5}$$

The δ_{ip}-term gives

$$\sigma_2\tau_2\tau_3\kappa_1\epsilon_{ijk}. \tag{4.6}$$

The second term with the ϵ_{ipl} vanishes because

$$N^T_B\sigma_2\sigma_l\tau_2\tau_3N_A = 0, \tag{4.7}$$

the reason being the Pauli exclusion principle.

The κ_0 contribution is

$$(B)\ \ P^i_{A'B}\kappa_0\sigma_p\epsilon_{pjk} = \frac{1}{\sqrt{8}}\sigma_2\sigma_i\tau_2\kappa_0\sigma_p\epsilon_{pjk}$$
$$= \frac{1}{\sqrt{8}}\kappa_0\tau_2\sigma_2(\delta_{ip} + i\epsilon_{ipl}\sigma_l)\epsilon_{pjk}, \tag{4.8}$$

where the δ_{ip}-term vanishes because of the Pauli exclusion principle ($N_B^T\tau_2\sigma_2 N_A = 0$). The other term contains $\tau_2\sigma_2\sigma_i$ which corresponds to a ${}^3S_1$ state and when projected onto the ${}^1S_0$ initial NN state gives zero.

So the only term that survives is the one appearing in equation (4.6) yielding the following

$$i\mathcal{M}_{(a)} = \frac{4}{\sqrt{8}}\sqrt{Z_d}\,\varepsilon^{*^i}_{(d)}\,(-ig^{({}^3S_1)})\frac{i}{(-B)}\frac{e}{2M}q_j\varepsilon^{*^k}_{(\gamma)}\epsilon^{ijk}\kappa_1 N^T\sigma_2\tau_2\tau_3 N. \tag{4.9}$$

Upon substituting $g^{({}^3S_1)} = \sqrt{\frac{8\pi}{M^2 r^{({}^3S_1)}}}$ and $Z_d = \sqrt{\frac{\gamma r^{({}^3S_1)}}{1-\gamma r^{({}^3S_1)}}}$, we arrive at

$$i\mathcal{M}_{(a)} = -\frac{2e}{M}\sqrt{\frac{\pi}{\gamma^3}}\frac{1}{\sqrt{1-\gamma r^{({}^3S_1)}}}\kappa_1\epsilon^{ijk}\varepsilon^{*^i}_{(d)}q^j\varepsilon^{*^k}_{(\gamma)}(N^T\sigma_2\tau_2\tau_3 N). \tag{4.10}$$

From equation (4.10), one can read off

$$Y_{(a)} = \frac{2}{M}\sqrt{\frac{\pi}{\gamma^3}}\frac{1}{\sqrt{1-\gamma r^{({}^3S_1)}}}\kappa_1. \tag{4.11}$$

One-loop contribution: diagram (b) in figure 4.1

The deuteron has spin +1 and orbital angular momentum $L = 0$. So it's in a spin triplet state with $S = 1$. Using the ${}^{2S+1}L_J$ notation where S is spin angular momentum, L is orbital angular momentum, and $J = L + S$ is total angular momentum, the deuteron state is ${}^3S_1$. In diagram (b) of figure 4.1, the photon couples to the nucleon via a magnetic coupling $\sigma_i\epsilon_{ijk}\partial_j A_k$ which takes away spin angular momentum. Thus the initial NN state must be in a relative ${}^1S_0$. Also both dibaryon-nucleon vertices before the photon coupling correspond to a ${}^1S_0$ state. The cross-section is being calculated at threshold energy $E = 0$. Keeping all of the above information in mind, we

can now write down the expression for the invariant amplitude as

$$
\begin{aligned}
i\mathcal{M}_{(b)} &= 8\,\sqrt{Z_d}\,\varepsilon^{*i}_{(d)}\,[-ig^{(^3S_1)}\,N_A(P_i)_{AB}N_B]\,\frac{e}{2M}q_j\delta_{km}N^\dagger_C[(\kappa_0+\tau_3\kappa_1)\,\sigma_p\epsilon_{pjm}]_{CD}N_D\,\varepsilon^{*m}_{(\gamma)} \\
&\times\int\frac{d^4k}{(2\pi)^4}\,\frac{i}{[k_0-\frac{\vec{k}^2}{2M}+i\epsilon]}\,\frac{i}{[k_0-B-\frac{(\vec{k}-\vec{B})^2}{2M}+i\epsilon]}\,\frac{i}{[-k_0-\frac{\vec{k}^2}{2M}+i\epsilon]} \\
&\times[-ig^{(^1S_0)}\,N^\dagger_E(P^\dagger_a)_{EF}N^\dagger_F]\frac{4\pi}{Mg^2_{(^1S_0)}}\frac{i}{\mu+\frac{4\pi}{Mg^2_{(^1S_0)}}\Delta}\,[-ig^{(^1S_0)}\,N^TP_aN], \qquad (4.12)
\end{aligned}
$$

where $B\simeq 2.2$ MeV is the deuteron binding energy which is taken away by the emitted photon. Thus the photon is also released with linear momentum $\vec{B}$. The factor of '8' is the symmetry factor of diagram (b).

Rearranging some terms we get

$$
\begin{aligned}
i\mathcal{M}_{(b)} &= 8\,\sqrt{Z_d}\,\varepsilon^{*i}_{(d)}\,[-ig^{(^3S_1)}\,(P_i)_{AB}]\,\frac{e}{2M}q_j\delta_{km}[(\kappa_0+\tau_3\kappa_1)\,\sigma_p\epsilon_{pjm}]_{BD}\,\varepsilon^{*m}_{(\gamma)} \\
&\times\int\frac{d^4k}{(2\pi)^4}\,\frac{i}{[k_0-\frac{\vec{k}^2}{2M}+i\epsilon]}\,\frac{i}{[k_0-B-\frac{(\vec{k}-\vec{B})^2}{2M}+i\epsilon]}\,\frac{i}{[-k_0-\frac{\vec{k}^2}{2M}+i\epsilon]} \\
&\times[-ig^{(^1S_0)}\,(P^\dagger_a)_{DA}]\frac{4\pi}{Mg^2_{(^1S_0)}}\frac{i}{\mu+\frac{4\pi}{Mg^2_{(^1S_0)}}\Delta}\,[-ig^{(^1S_0)}\,N^TP_aN] \\
&= 8\,\frac{1}{8}\sqrt{Z_d}\,\varepsilon^{*i}_{(d)}\,[-ig^{(^3S_1)}]\,\frac{e}{2M}q_j\delta_{km}\epsilon_{pjm}\,\varepsilon^{*m}_{(\gamma)} \\
&\times\int\frac{d^4k}{(2\pi)^4}\,\frac{i}{[k_0-\frac{\vec{k}^2}{2M}+i\epsilon]}\,\frac{i}{[k_0-B-\frac{(\vec{k}-\vec{B})^2}{2M}+i\epsilon]}\,\frac{i}{[-k_0-\frac{\vec{k}^2}{2M}+i\epsilon]}\,[-ig^{(^1S_0)}] \\
&\times\frac{4\pi}{Mg^2_{(^1S_0)}}\frac{i}{\mu+\frac{4\pi}{Mg^2_{(^1S_0)}}\Delta}\,[-ig^{(^1S_0)}\,N^TP_aN]\,Tr[\sigma_2\sigma_i\sigma_p\sigma_2]\times Tr[\tau_2(\kappa_0+\tau_3\kappa_1)\tau_a\tau_2]
\end{aligned}
\qquad (4.13)
$$

Three-Propagator Integral:

In order to complete the calculation, we have to evaluate the following three-propagator integral:

$$
I=\int\frac{d^4k}{(2\pi)^4}\,\frac{1}{[k_0-\frac{\vec{k}^2}{2M}+i\epsilon]}\,\frac{1}{[k_0-B-\frac{(\vec{k}-\vec{B})^2}{2M}+i\epsilon]}\,\frac{1}{[-k_0-\frac{\vec{k}^2}{2M}+i\epsilon]} \qquad (4.14)
$$

To achieve the task of evaluating the integral in equation (4.14), we follow these steps. We first perform the k_0 integration by closing the contour in a convenient way which

would be in the upper-half complex plane. Integrating over k_0 gives

$$I = i \int \frac{d^3k}{(2\pi)^3} \frac{1}{[-\frac{\vec{k}^2}{M} + i\epsilon]} \frac{1}{[-\frac{\vec{k}^2}{2M} - B - \frac{1}{2M}(\vec{k}^2 - 2\vec{k}\cdot\vec{B} + \vec{B}^2) + i\epsilon]}. \tag{4.15}$$

After rearranging some terms and neglecting the term $\frac{B^2}{4M}$ in comparison with B (knowing that B=2.2 MeV and M=940 MeV)we get the integral

$$I = -iM^2 \int \frac{d^3k}{(2\pi)^3} \frac{1}{[\vec{k}^2 - i\epsilon]} \frac{1}{[MB + (\vec{k} - \frac{\vec{B}}{2})^2 - i\epsilon]}. \tag{4.16}$$

The next step is to introduce Fourier transforms $f(\vec{r})$ and $g(\vec{r})$ of the propagators such that

$$FT[f(\vec{r}), \vec{p}] = \frac{1}{\vec{p}^2 - i\epsilon}, \tag{4.17}$$

$$FT[g(\vec{r}), \vec{p}] = \frac{1}{MB - \vec{p}^2 - i\epsilon}. \tag{4.18}$$

In general,

$$FT[h(\vec{r}), \vec{p}] = \int d^3r \; h(\vec{r}) e^{-i\vec{p}\cdot\vec{r}}, \tag{4.19}$$

and it can be shown that

$$g(\vec{r}) = \frac{1}{4\pi} \frac{e^{-\sqrt{MB}r}}{r}. \tag{4.20}$$

Taking the limit $B \longrightarrow 0$ in $g(\vec{r})$ gives $f(\vec{r}) = \frac{1}{4\pi r}$. Before I continue with the evaluation of the integral, let me take a few lines to show that

$$g(\vec{r}) = \frac{1}{4\pi} \frac{e^{-\sqrt{MB}r}}{r}. \tag{4.21}$$

In order to do this, we need to insert

$$g(\vec{r}) = \frac{1}{4\pi} \frac{e^{-\sqrt{MB}r}}{r} \tag{4.22}$$

into

$$\int d^3r \; g(\vec{r}) \; e^{-i\vec{p}\cdot\vec{r}} \tag{4.23}$$

and show that it's equal to $\frac{1}{MB+\vec{p}^2-i\epsilon}$.

Plugging in $g(\vec{r})$ from equation (4.22) into equation (4.23) gives

$$\begin{aligned}\int d^3r\ \frac{e^{-\sqrt{MB}r}}{4\pi r}\ e^{-i\vec{p}\cdot\vec{r}} =& \frac{1}{2}\ \int dr\ d\theta\ \sin\theta\ re^{-\sqrt{MB}r}\ e^{-ipr\cos\theta} \\ =& \frac{i}{2p}\ \int_0^\infty dr\ [e^{-(\sqrt{MB}+ip)r}\ -\ e^{-(\sqrt{MB}-ip)r}] \\ =& \frac{i}{2p}\ (\frac{1}{\sqrt{MB}+ip}\ -\ \frac{1}{\sqrt{MB}-ip}) \\ =& \frac{i}{2p}\ (\frac{-2ip}{MB+p^2}) \\ =& \frac{1}{MB+p^2}\end{aligned} \tag{4.24}$$

as claimed above.

We now rewrite the propagators in the integral I in terms of their Fourier transforms. So,

$$I = -iM^2\ \int \frac{d^3k}{(2\pi)^3}[\int \frac{d^3r}{4\pi r}e^{-i\vec{k}\cdot\vec{r}}\ \int \frac{d^3r'}{4\pi r'}e^{-\sqrt{MB}r'}e^{-i(\vec{k}-\frac{\vec{B}}{2})\cdot\vec{r'}}]. \tag{4.25}$$

This can be rearranged to give

$$I = -iM^2\ \int \frac{d^3k}{(2\pi)^3}e^{i\vec{k}\cdot(-\vec{r}-\vec{r'})}\ \int \frac{d^3r\ d^3r'}{16\pi^2}\ \frac{1}{r}\ \frac{e^{-\sqrt{MB}r'}}{r'}\ e^{i\frac{\vec{B}}{2}\cdot\vec{r'}}. \tag{4.26}$$

First, we perform the k integration and then the remaining integrations over r and r'. Notice that the integral over k gives a $\delta^3(\vec{r}+\vec{r'})$.

After integrating over r' using the Dirac delta function, we get

$$I = -iM^2\ \int \frac{d^3r}{16\pi^2}\ \frac{1}{r^2}\ e^{-\sqrt{MB}r'}\ e^{-i\frac{\vec{B}}{2}\cdot\vec{r'}}. \tag{4.27}$$

Next, we integrate over the angles ϕ and θ which are both simple integrations to arrive at

$$I = \frac{-iM^2}{2\pi B}\ \int_0^\infty\ dr\ \frac{e^{-\gamma r}}{r}\ \sin(\frac{Br}{2}), \tag{4.28}$$

where $\gamma = \sqrt{MB}$. Using

$$\int_0^\infty\ dr\ \frac{e^{-\gamma r}}{r}\ \sin(\frac{Br}{2}) = \arctan(\frac{B}{2\gamma}), \tag{4.29}$$

we find that

$$I = \frac{-iM^2}{2\pi B}\ \arctan(\frac{B}{2\gamma}). \tag{4.30}$$

Expanding the arctan [$\arctan(x) = x - \frac{x^3}{3} + ...$] and keeping the lowest order term gives

$$I = \frac{-iM^2}{2\pi B}(\frac{B}{2\gamma}) = \frac{-iM^2}{4\pi\gamma}. \tag{4.31}$$

Going back to the one loop diagram

For ease of reading, we report below the amplitude expression of Eq.(4.13)

$$\begin{aligned} i\mathcal{M}_{(b)} = & \sqrt{Z_d}\ \varepsilon^{*^i}_{(d)}\ [-ig^{(^3S_1)}]\ \frac{e}{2M} q_j \delta_{km} \epsilon_{pjm}\ \varepsilon^{*^m}_{(\gamma)} \\ & \int \frac{d^4k}{(2\pi)^4}\ \frac{i}{[k_0 - \frac{\vec{k}^2}{2M} + i\epsilon]}\ \frac{i}{[k_0 - B - \frac{(\vec{k}-\vec{B})^2}{2M} + i\epsilon]}\ \frac{i}{[-k_0 - \frac{\vec{k}^2}{2M} + i\epsilon]}\ [-ig^{(^1S_0)}] \\ & \frac{4\pi}{Mg^2_{(^1S_0)}} \frac{i}{\mu + \frac{4\pi}{Mg^2_{(^1S_0)}}\Delta}\ [-ig^{(^1S_0)}\ N^T P_a N]\ Tr[\sigma_2\sigma_i\sigma_p\sigma_2] \times Tr[\tau_2(\kappa_0 + \tau_3\kappa_1)\tau_a\tau_2]. \end{aligned} \tag{4.32}$$

Now we plugin the value of the three-propagator integral given in Eq.(4.30) into the amplitude expression given above to obtain

$$\begin{aligned} i\mathcal{M}_{(b)} = & \sqrt{Z_d}\ \varepsilon^{*^i}_{(d)}\ [-ig^{(^3S_1)}]\ \frac{e}{2M} q_j \epsilon_{pjk}\ \varepsilon^{*^k}_{(\gamma)}\ (\frac{-M^2}{4\pi\gamma})[-ig^{(^1S_0)}] \\ & \frac{4\pi}{Mg^2_{(^1S_0)}} \frac{i}{\mu + \frac{4\pi}{Mg^2_{(^1S_0)}}\Delta}\ [-ig^{(^1S_0)}\ N^T P_a N]\ 2\delta_{ip}\ 2\kappa_1\delta_{3a} \end{aligned} \tag{4.33}$$

Using $Z_d = \frac{\gamma r^{(^3S_1)}}{1 - \gamma r^{(^3S_1)}}$, $g^2 = \frac{8\pi}{M^2 r}$, $\Delta = \frac{2}{Mr}(\frac{1}{a} - \mu)$ and $P_a = \frac{1}{\sqrt{8}}\tau_2\tau_a\sigma_2$, the one-loop invariant amplitude becomes

$$i\mathcal{M}_{(b)} = \frac{2}{M}\sqrt{\frac{\pi}{\gamma^3}}\ \frac{1}{\sqrt{1 - \gamma r^{(^3S_1)}}}\ \gamma e\ a^{(^1S_0)}\ \kappa_1\ q_j\ \epsilon_{ijk}\ \varepsilon^{*^k}_{(\gamma)}\ \varepsilon^{*^i}_{(d)}\ N^T\tau_2\tau_3\sigma_2 N. \tag{4.34}$$

From the above amplitude (Eq.(4.34)), we can read off

$$Y_{(b)} = -\frac{2}{M}\sqrt{\frac{\pi}{\gamma^3}}\ \frac{1}{\sqrt{1 - \gamma r^{(^3S_1)}}}\ \kappa_1\ \gamma\ a^{(^1S_0)}. \tag{4.35}$$

The total amplitude

$$\begin{aligned} Y &= Y_{(a)} + Y_{(b)} \\ &= -\frac{2}{M}\sqrt{\frac{\pi}{\gamma^3}}\frac{1}{\sqrt{1-\gamma r^{(^3S_1)}}}\kappa_1(\gamma a^{(^1S_0)} - 1). \end{aligned} \tag{4.36}$$

4.2 From amplitude to cross-section

The cross-section is given by Eq. (4.1), and the invariant amplitude by equation (4.2) where Y has already been calculated (Eq. (4.36)). The next step is to evaluate $|\mathcal{M}|^2$, so we need the nucleon and proton fields, N_n and N_p, respectively. They are given by

$$N_n = \frac{1}{2}(\mathbb{1} - \tau_3)N, \tag{4.37}$$

and

$$N_p = \frac{1}{2}(\mathbb{1} + \tau_3)N. \tag{4.38}$$

Next, we have

$$N_n^T O N_p = N^T \frac{1}{2}(\mathbb{1} - \tau_3)O\frac{1}{2}(\mathbb{1} + \tau_3)N, \tag{4.39}$$

where $O = \tau_2\tau_3\sigma_2$. Plugging in equation (4.39) into $|\mathcal{M}|^2$ gives

$$\begin{aligned} |\mathcal{M}|^2 = \mathcal{M}\mathcal{M}^\dagger = [ieY\epsilon^{ijk}\varepsilon^{*^i}_{(d)}q^j\varepsilon^{*^k}_{(\gamma)}N^T_{A'}\frac{1}{2}(\mathbb{1}-\tau_3)_{A'A}(\tau_2\tau_3\sigma_2)_{AB}\frac{1}{2}(\mathbb{1}+\tau_3)_{BB'}N_{B'}] \\ \times [-ieY\epsilon^{abc}\varepsilon^{*^a}_{(d)}q^b\varepsilon^{*^c}_{(\gamma)}N^\dagger_{C'}\frac{1}{2}(\mathbb{1}+\tau_3)_{C'C}(\tau_3\tau_2\sigma_2)_{CD}\frac{1}{2}(\mathbb{1}-\tau_3)_{DD'}(N^T)^\dagger_{D'}] \end{aligned} \tag{4.40}$$

where A', A, B', B, etc are combined spin-isospin indices carried by the nucleon fields. Using

$$\sum_{spin,isospin} N^T_{A'}(N^T)^\dagger_{D'} = \delta_{A'D'} \tag{4.41}$$

and

$$\sum_{spin,isospin} N_{B'}N^\dagger_{C'} = \delta_{B'C'}, \tag{4.42}$$

we obtain

$$\sum_{spin,isospin} |\mathcal{M}|^2 = \frac{e^2Y^2}{16}\sum\{\epsilon^{ijk}\epsilon^{abc}\varepsilon^{*^i}_{(d)}\varepsilon^{*^a}_{(d)}\varepsilon^{*^k}_{(\gamma)}\varepsilon^{*^c}_{(\gamma)}q^j q^b \times Tr[(\mathbb{1}-\tau_3)(\tau_2\tau_3\sigma_2) (\mathbb{1}+\tau_3)(\mathbb{1}+\tau_3)(\tau_3\tau_2\sigma_2)(\mathbb{1}-\tau_3)]\}. \tag{4.43}$$

Next, we use

$$\sum \varepsilon^{*^i}_{(d)}\varepsilon^{*^a}_{(d)} = (-\delta_{ia} + \frac{k^i_{(d)}k^a_{(d)}}{M^2_{(d)}}) \tag{4.44}$$

and

$$\sum \varepsilon^{*^k}_{(\gamma)}\varepsilon^{*^c}_{(\gamma)} = (-\delta_{kc} + \frac{q^k q^c}{q^2}) \tag{4.45}$$

where $k_{(d)}$ and q are the deuteron and photon momenta, respectively. $M_{(d)}$ is the deuteron mass.

Since we are calculating the cross-section of unpolarized $n(p,d)\gamma$, we will need to average over initial spins which introduces a factor of (1/4). So we arrive at

$$\frac{1}{4}\sum |\mathcal{M}|^2 = \frac{1}{4}\frac{e^2Y^2}{16}\epsilon^{ijk}\epsilon^{abc}(-\delta_{ia} + \frac{k^i_{(d)}k^a_{(d)}}{M^2_{(d)}})(-\delta_{kc} + \frac{q^k q^c}{q^2})q^j q^b \times 4Tr[(\mathbb{1}-\tau_3)(\tau_2\tau_3\sigma_2) (\mathbb{1}+\tau_3)(\tau_3\tau_2\sigma_2)]. \tag{4.46}$$

After a couple lines of algebraic manipulations, we get to the following expression

$$\frac{1}{4}\sum |\mathcal{M}|^2 = e^2Y^2q^2. \tag{4.47}$$

Knowing that the differential cross-section at threshold is given by (see e.g. Ref. [37])

$$\frac{d\sigma}{d\Omega} = \frac{\gamma^2+p^2}{16\pi^2 p}\sum |\mathcal{M}|^2, \tag{4.48}$$

where $\gamma^2 = MB$, B being the binding energy of the deuteron and also the energy of the outgoing photon, p is the momentum of the proton in the center of mass (CM) frame, and M is the nucleon mass.

After substituting equation (4.47) for $\sum |\mathcal{M}|^2$, the total cross-section is

$$\sigma = 4\pi e^2\frac{\gamma^2+p^2}{16\pi^2 p}q^2Y^2. \tag{4.49}$$

where $q = \frac{p^2+\gamma^2}{M}$ is the outgoing photon momentum, which when inserted in the expression above yields the final LO result [32]

$$\sigma = \frac{\alpha(\gamma^2+p^2)^3}{M^2 p} Y^2 \tag{4.50}$$

with $\alpha = \frac{e^2}{4\pi}$.

Having derived the expression for the $n(p,d)\gamma$ cross-section (Eq. (4.50)), let us find a numerical value for σ_{LO}. Inserting the following:

$\alpha = \frac{1}{137}$, $\gamma = \sqrt{MB} \approx 45.68$ MeV $= 0.23$ fm^{-1}, $r^{(^3S_1)}$=1.75 fm, $a^{(^1S_0)}$=-23.71 fm, $\kappa_1 \approx 2.35$, $p = \frac{p_{lab}}{2} = 3.45 \times 10^{-3}$ MeV ($p_{lab} = M\beta_{lab} = M\frac{v_{lab}}{c}$ with $v_{lab} = 2200$ m/s) into Eq. (4.50) where Y is given by Eq (4.36) yields a value of

$$\sigma_{LO} \approx \ 49.4 \text{ fm}^2 = 494 \text{ mb} \tag{4.51}$$

Note that since $p \ll \gamma$, I have neglected the p^2 term in the numerator of Eq. (4.50) while performing the numerical calculation. Setting $c = \hbar = 1$, we can use 1 MeV=$\frac{1}{197.3 \text{ fm}}$.

Brief discussion of our result

Our LO calculation of $n(p,d)\gamma$ cross-section using EFT($\not\pi$) with dibaryon fields yielded a value of $\sigma_{LO} = 494$ mb. This is approximately 1.5 times greater than the experimental value which is $\sigma_{exp} = 334.2 \pm 0.5$ mb [39]. The energy at which we calculated the cross-section is 0.025 eV which is the kinetic energy of a thermal neutron. This energy corresponds to the most probable speed of a Maxwell-Boltzmann distribution at room temperature.

The expansion parameter is $Q \sim \frac{\gamma}{M_\pi}$ where the deuteron binding momentum γ is a typical momentum scale, and M_π is the pion mass. The two LO diagrams (Fig. 4.1) contributing to the amplitude Y are of $O(Q^0)$. Since our cross-section is a "simple" LO computation involving only two diagrams, we can't expect to do better. At next-to-leading order (NLO), $O(Q)$, there's a contribution from one diagram which

corresponds to a four-nucleon operator coupling to the magnetic field

$$e\frac{L_1}{M\sqrt{r(^1S_0)r(^3S_1)}}t^{j\dagger}s_3B_j$$

where t_j and s_a are the dibaryon fields in the $^3S_1$ and $^1S_0$, respectively. The coefficient L_1 is to be fixed either from QCD or experimentally (see e.g. Ref. [32]). There are no other diagrams that enter at NLO. So, in order to improve our result, we can calculate the contributions of higher-order diagrams which has actually been done by for example Rupak [2] and Chen and Savage [29].

Chapter 5

Conclusion

In this thesis, I have shown the details of the unpolarized $n(p,d)\gamma$ cross-section calculation up to LO employing the framework of EFT($\not\pi$) with dibaryon fields. The predicted numercial value is $\sigma_{LO} = 494$ mb. The cross-section calculation presented here is only a 'simple' application of EFT. Further work using EFTs has been done. The $np \to d\gamma$ cross-section has been calculated to higher orders [1, 2, 3]. The inverse reactions $\gamma d \to np$ and $\vec{\gamma} d \to np$ have also been studied using EFT($\not\pi$) with dibaryon fields [3]. Furthermore, EFT has been applied to study the polarized $n(p,d)\gamma$ reaction at threshold [4] and parity-violating effects [35, 36].

The $n(p,d)\gamma$ reaction was put in the context of BBN. The fact that deuterium formation is very sensitive to the density of baryonic matter (Ω_b) in the universe, its abundance provides a measure of Ω_b (see for example [15]). Deuteron production cross-section enters in Ω_b calculations, so computing this cross-section to higher precision is a big matter of interest. A precision calculation of $n(p,d)\gamma$ cross-section at BBN energies was done by Rupak [2].

As mentioned earlier, BBN is one of the four pillars upon which the validity of the Big Bang model rests. The accuracy of most BBN predictions, for instance, light element abundances, provides supportive evidence of the standard big bang scenario. However, it is worth mentioning that BBN is being used to probe for new physics. In their recent paper, Pospelov and Pradler explore nonstandard cosmological and particle physics scenarios by showing how new physics can modify standard BBN [16].

Bibliography

[1] J. -W. Chen, G. Rupak and M. J. Savage, Phys. Lett. B 464, 1 (1999) [nucl-th/9905002].

[2] G. Rupak, Nucl. Phys. A 678, 405 (2000) [nucl-th/9911018].

[3] S. Ando, R. H. Cyburt, S. W. Hong and C. H. Hyun, Phys. Rev. C 74, 025809 (2006) [nucl-th/0511074].

[4] T. -S. Park, K. Kubodera, D. -P. Min and M. Rho, Phys. Lett. B 472, 232 (2000) [nucl-th/9906005].

[5] G. Lemaitre, "The Primeval Atom, An Essay on Cosmogony," New York, Van Nostrand 1950, 186p

[6] R. A. Alpher, H. Bethe and G. Gamow, Phys. Rev. 73, 803 (1948).

[7] S. Weinberg, "The First Three Minutes. A Modern View of the Origin of the Universe," Muenchen 1977, 269p

[8] R. A. Alpher, J. W. Follin and R. C. Herman, Phys. Rev. 92, 1347 (1953).

[9] M. E. Burbidge, G. R. Burbidge, W. A. Fowler and F. Hoyle, Rev. Mod. Phys. 29, 547 (1957).

[10] A.G.W. Cameron, "Stellar Evolution, Nuclear Astrophysics, and Nucleogenesis" Chalk River 1957, 167p

[11] F. Hoyle and R. J. Tayler, Nature 203, 1108 (1964).

[12] P. J. E. Peebles, Astrophys. J. 146, 542 (1966).

[13] R. V. Wagoner, W. A. Fowler and F. Hoyle, Astrophys. J. 148, 3 (1967).

[14] H. Reeves, J. Andouze, W. A. Fowler and D. N. Schramm, Astrophys. J. 179, 909 (1973).

[15] S. Burles and D. Tytler, astro-ph/9803071.

[16] M. Pospelov and J. Pradler, Ann. Rev. Nucl. Part. Sci. 60, 539 (2010) [arXiv:1011.1054 [hep-ph]].

[17] B. Fields and S. Sarkar, astro-ph/0601514.

[18] K. A. Olive, Nucl. Phys. Proc. Suppl. 80, 79 (2000) [astro-ph/9903309].

[19] G. Steigman, Ann. Rev. Nucl. Part. Sci. 57, 463 (2007) [arXiv:0712.1100 [astro-ph]].

[20] S. Burles, K. M. Nollett and M. S. Turner, astro-ph/9903300.

[21] D. B. Kaplan, nucl-th/0510023.

[22] D. B. Kaplan, nucl-th/9506035.

[23] B. R. Holstein, Nucl. Phys. A 689, 135 (2001) [nucl-th/0010015].

[24] H. Georgi, Ann. Rev. Nucl. Part. Sci. 43, 209 (1993).

[25] A. Pich, hep-ph/9806303.

[26] D. R. Phillips, Czech. J. Phys. 52, B49 (2002) [nucl-th/0203040].

[27] M. E. Peskin and D. V. Schroeder, "An Introduction to quantum field theory," Reading, USA: Addison-Wesley (1995) 842 p

[28] J. C. Collins, "Renormalization. An Introduction To Renormalization, The Renormalization Group, And The Operator Product Expansion," Cambridge, Uk: Univ. Pr. (1984) 380p

[29] J. -W. Chen and M. J. Savage, Phys. Rev. C 60, 065205 (1999) [nucl-th/9907042].

[30] J. -W. Chen, G. Rupak and M. J. Savage, Nucl. Phys. A 653, 386 (1999) [nucl-th/9902056].

[31] D. B. Kaplan, Nucl. Phys. B 494, 471 (1997) [nucl-th/9610052].

[32] S. R. Beane and M. J. Savage, Nucl. Phys. A 694, 511 (2001) [nucl-th/0011067].

[33] D. B. Kaplan, M. J. Savage and M. B. Wise, Phys. Lett. B 424, 390 (1998) [nucl-th/9801034].

[34] S. Scherer and M. R. Schindler, hep-ph/0505265.

[35] D. B. Kaplan, M. J. Savage, R. P. Springer and M. B. Wise, Phys. Lett. B 449, 1 (1999) [nucl-th/9807081].

[36] J. W. Shin, S. Ando and C. H. Hyun, Phys. Rev. C 81, 055501 (2010) [arXiv:0907.3995 [nucl-th]].

[37] S. Christlmeier, "Electrodisintegration of the Deuteron in Effective Field Theory," Diploma thesis, TU Muenchen (Germany), 2004

[38] G. 't Hooft and M. J. G. Veltman, Nucl. Phys. B 44, 189 (1972).

[39] A.E. Cox, S.A.R. Wynchank and C.H. Collie, Nucl. Phys. 74, 497 (1965).